



MHD simulation for the interaction of an interplanetary shock with the Earth's magnetosphere

A. A. Samsonov,¹ D. G. Sibeck,² and J. Imber³

Received 10 July 2007; revised 25 September 2007; accepted 10 October 2007; published 28 December 2007.

[1] The global BATS-R-US MHD code is used to simulate the interaction of a moderately strong interplanetary shock with the Earth's magnetosphere. The model predicts the propagation of a transmitted fast shock through the magnetosheath and magnetosphere and the reflection of this shock from the inner numerical boundary. The reflected fast shock propagates sunward through the dayside magnetosphere and magnetosheath. The passage of the transmitted shock causes the bow shock and magnetopause to move inward, while the passage of the reflected fast shock causes these boundaries to move outward, consistent with previously reported in situ observations. A supplementary study employing a one-dimensional MHD model addresses the interaction of the forward fast shock with the plasmapause. This study demonstrates that most of the energy associated with the fast shock energy penetrates into the plasmasphere. Consequently, the transmitted fast wave must reach the ionosphere, produce the well known sudden impulse signatures, and then be reflected due to the shielding effects of ionospheric currents. The predictions of the numerical simulations are consistent with observations of the dayside geosynchronous magnetic field.

Citation: Samsonov, A. A., D. G. Sibeck, and J. Imber (2007), MHD simulation for the interaction of an interplanetary shock with the Earth's magnetosphere, *J. Geophys. Res.*, 112, A12220, doi:10.1029/2007JA012627.

1. Introduction

[2] Solar wind conditions play a dominant role in determining the level of geomagnetic activity. High-speed solar wind streams and coronal mass ejections launch interplanetary (IP) shocks which propagate antisunward through the solar wind with supersonic velocities. When the IP shocks reach the magnetosphere, they initiate global magnetospheric disturbances. Geomagnetic sudden impulse or sudden commencement signatures are very clear global phenomena caused by IP shocks [e.g., *Nishida*, 1978; *Araki*, 1994].

[3] IP shocks are usually fast forward MHD shocks. The interaction of an IP shock with the magnetosphere follows several particular phases, including the interaction of the IP shock with the bow shock, the interaction of the IP shock with the magnetopause, the transmission of the IP shock into the magnetosphere as a fast mode wave, modifications of the field-aligned and ionospheric current systems, and magnetic disturbances observed on the ground. In this paper we will focus on the IP shock interaction with the bow shock and magnetopause, without addressing the ionospheric response.

[4] The interaction of IP shocks with the Earth's bow shock has long been a topic for theoretical, laboratory, and

observational study [*Ivanov*, 1964; *Dryer et al.*, 1967; *Shen and Dryer*, 1972; *Dryer*, 1973; *Grib et al.*, 1979; *Zhuang et al.*, 1981; *Grib*, 1982; *Pushkar et al.*, 1991; *Grib and Pushkar*, 2006]. More recently, one- and three-dimensional numerical MHD simulations for the IP-bow shock interaction have been employed [*Yan and Lee*, 1996; *Samsonov et al.*, 2006]. Figure 1 illustrates the results of an IP-bow shock interaction in the case when the IP shock propagates radially outward from the Sun and the interplanetary magnetic field (IMF) has a spiral orientation. The interaction launches a fast shock (FS) into the magnetosheath which propagates at a speed lower than that of the solar wind IP shock [*Samsonov et al.*, 2006], in agreement with predictions from the Rankine-Hugoniot conditions and observations [*Koval et al.*, 2005, 2006]. The bow shock, a reverse fast shock, moves earthward with a velocity $\sim 100 \text{ km s}^{-1}$. Three new discontinuities appear downstream from the bow shock in addition to the FS: a forward slow expansion wave (SEW), a contact discontinuity (CD), and a reverse slow shock (SS). Because the propagation velocities of these three discontinuities are very similar, they cannot be distinguished in the results of 3-D simulations. Instead, they take the form of a single discontinuity where the magnetic field strength and density increase, the temperature decreases, and the velocity remains unchanged [*Samsonov et al.*, 2006].

[5] Rankine-Hugoniot conditions can also be used to study the interaction of an IP shock with a tangential discontinuity (TD) magnetopause. The interaction for typical shock conditions sets the magnetopause moving inward at speeds greater than 200 km s^{-1} and launches a transmitted fast shock into the magnetosphere that propagates with a

¹Institute of Physics, St. Petersburg State University, St. Petersburg, Russia.

²NASA Goddard Space Flight Center, Greenbelt, Maryland, USA.

³University of Oxford, Oxford, UK.

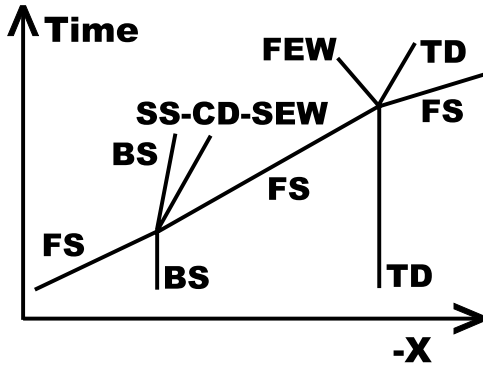


Figure 1. Predictions obtained from the Rankine-Hugoniot relations at the Sun-Earth line. Interaction of interplanetary fast shock (FS) with the bow shock (BS) for a case with $\angle(\mathbf{B}_{IMF}, \mathbf{V}) = 45^\circ$ results in a forward FS, a combination of forward slow expansion wave (SEW), contact discontinuity (CD), and reversed slow shock (SS), and a modified bow shock. Interaction of the FS with the magnetopause (it is usually assumed to be a tangential discontinuity TD) results in a FS propagating inside the magnetosphere, a modified TD, and a reflected fast expansion wave (FEW) moving sunward in the magnetosheath.

velocity on the order of 1500 km s^{-1} . *Grib* [1972, 1973] predicted that the interaction would also launch an outward-propagating fast expansion wave (FEW) into the magnetosheath.

[6] *Ridley et al.* [2006] presented the results of a global simulation employing the BATS-R-US MHD code for the interaction of an extremely strong IP shock with the magnetosphere. The transmitted IP shock propagates through the magnetosheath and magnetosphere, then reflects from the inner numerical boundary and moves outward. *Ridley et al.* [2006] assumed that the reflection boundary corresponded to the plasmopause. The transmitted IP shock propagated around the flanks of the magnetosphere toward the magnetotail. The dayside bow shock moved inward until it interacted with the reflected shock.

[7] *Guo et al.* [2005] used a PPMLR-MHD code to study the interaction of IP shocks with the magnetosphere. They considered two cases: one when the shock normal lies along the Sun-Earth line, the other when the angle between the shock normal and the Sun-Earth line is 60° . Despite differing transitions, the system evolved to nearly the same final quasi-steady state configuration in both cases.

[8] *Lee and Hudson* [2001] used a 3-D dipole model for the magnetosphere to study a similar problem, namely the propagation of a sudden impulse associated with the IP shock inside the magnetosphere. To simulate the response, they invoked an abrupt variation in the electric field at the outer boundary of their model, the magnetopause. Their results indicate that most of the impulse energy penetrates the plasmopause to excite strong low-frequency pulsations in the plasmasphere, but that a small portion of the initial impulse is reflected from the plasmopause and returns to the outer boundary.

[9] Despite these studies, many aspects of the interaction of solar wind shocks with the magnetosphere remain unclear. We can (and will) use existing global MHD models to predict the motion of the bow shock [*Šafránková et al.*, 2007] and corresponding signatures at geosynchronous orbit [*Andreeva and Perech*, 2007]. However, there are some questions that contemporary global MHD models cannot address. Only a model employing a realistic plasmasphere can be used to estimate the energy fluxes transmitted into the plasmasphere and reflected back into the outer magnetosphere when an interplanetary shock strikes.

[10] In the next section, we present a short description of the MHD model and the initial and boundary conditions. Section 3 presents results from the global MHD model. Section 4 introduces a simple 1-D MHD model at the Sun-Earth line to address the nature of the reflecting boundary. Section 5 contains further discussions of this topic, quantitative estimations of energy transmission through the magnetospheric boundaries and comparison with observations. As usual, the last section presents our conclusions.

2. Numerical Model

[11] This work employs the global BATS-R-US code to simulate the solar wind-magnetosphere interaction [*Powell et al.*, 1999]. The BATS-R-US code solves the MHD equations with a finite volume discretization in a 3-D block-adaptive Cartesian grid using conservative variables. As usual for global codes, the supersonic solar wind conditions are imposed on a plane perpendicular to the Sun-Earth line (X axis) upstream from the bow shock. There is an outflow boundary far downstream in the magnetotail. The inner numerical boundary is located about $3 R_E$ from the Earth. The boundary conditions allow no mass flux through this inner boundary and reflective boundary conditions are used for the mass density and the thermal pressure [*Song et al.*, 1999]. The magnetic field near the inner boundary is determined primarily by the imposed terrestrial magnetic field [*Gombosi et al.*, 2003].

[12] As a basic approach, we use a version of the BATS-R-US code that is coupled to the Rice Convection Model (RCM) [*De Zeeuw et al.*, 2004]. The latter model includes a representation of the inner magnetosphere and its connection to the ionosphere. We compared results from the BATS-R-US code with and without the RCM coupling, but found no significant differences. The resolution of the numerical grid has been enhanced in the dayside region near the Sun-Earth line, with the smallest computational cell $0.125 \times 0.125 \times 0.125 R_E^3$. The region with the finest resolution is a square with dimensions of $15 \times 15 R_E^2$ in the Y - Z plane situated between the terminator plane ($x = 0$) and the solar wind inflow boundary ($x = 20 R_E$). The grid spacing gradually increases with increasing $|y|$ and $|z|$.

[13] We simulate the interaction of a moderately strong forward fast shock in the solar wind with the Earth's magnetosphere. First, we find a quasi-stationary solution for the following initial solar wind conditions: $\rho_0 = 5 \text{ cm}^{-3}$, $B_0 = 5 \text{ nT}$, $T_0 = 2.4 \times 10^5 \text{ K}$, $V_0 = 400 \text{ km s}^{-1}$, $\theta_{BV} = 45^\circ$. Here, θ_{BV} is the angle between the magnetic field and the flow velocity, where the flow direction is along the $-X$ axis. All other parameters are used in their usual sense. We then impose an interplanetary shock with a shock normal in the

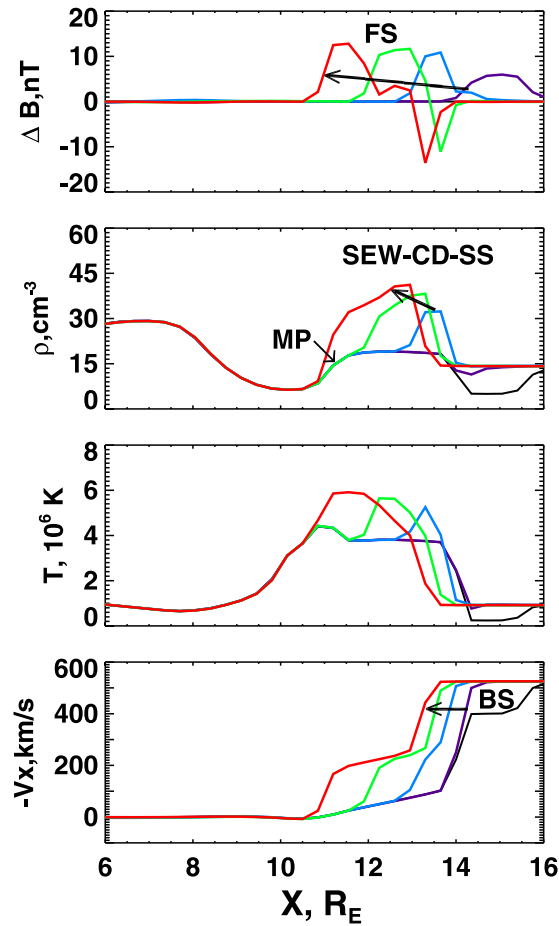


Figure 2. Profiles of the ΔB , density, temperature, and radial velocity at the Sun-Earth line in different moments. The $\Delta B = |B_n| - |B_{n-1}|$ is a time variation of the magnetic field magnitude during 15 seconds. Black, violet, blue, green and red colors correspond to $t = 60, 75, 90, 105, 120$ s (at moment $t = 0$ the IP shock has been launched at the solar wind boundary). MP, FS, and BS mean the magnetopause, the forward fast shock (IP shock) and the bow shock respectively. SEW-CD-SS is a combination of slow expansion wave, contact discontinuity, and reversed slow shock. Arrows show the motion of the discontinuities.

$-X$ direction. Solar wind parameters downstream from the shock are: $\rho_d = 14.2 \text{ cm}^{-3}$, $B_d = 11.3 \text{ nT}$, $T_d = 9.2 \cdot 10^5 \text{ K}$, $V_d = 525 \text{ km s}^{-1}$. From the Rankine-Hugoniot conditions, we obtain a shock velocity of 594 km s^{-1} .

3. Results of Global Modeling

[14] We begin by considering the evolution of MHD parameters along the Sun-Earth line, where the various discontinuities can be identified most easily. Figure 2 presents five profiles of ΔB , density, temperature, and V_x along the Sun-Earth line, each separated by 15 s. The profile for ΔB represents the difference between the present magnetic field magnitude and the magnetic field magnitude 15 s before. The figure illustrates the propagation of the IP shock through the bow shock and magnetosheath. We will use the

abbreviation FS throughout this work to indicate the transmitted IP shock propagating through the magnetosheath and magnetosphere toward the Earth. The passage of the shock through the magnetosheath enhances all four MHD parameters in Figure 2. In the final (red) profile, the position of the FS approximately coincides with the subsolar magnetopause at $x = 11 R_E$. In agreement with past work describing the SEW-CD-SS discontinuity [Samsonov *et al.*, 2006], there is a structure between the forward FS and the bow shock (BS) characterized by a density and magnetic field strength increase but a decrease of the temperature. The magnetopause (MP) and BS begin to move Earthward after the interaction with the IP shock in agreement with the Rankine-Hugoniot conditions.

[15] Figure 3 shows similar profiles for the next set of 15 s intervals. The FS propagates inward through the magnetosphere. In the final profile, it lies just outside the inner numerical boundary at $x = 3 R_E$. The MP and BS continue to move Earthward. Figure 4 shows the next set of 15 s profiles. A reflected fast shock (RFS) moves sunward, enhancing densities and magnetic field strengths, but diminishing Earthward velocities. This reflected shock is transmitted through the magnetopause into the magnetosheath. The passage of the RFS nearly stops the inward motion of the magnetopause.

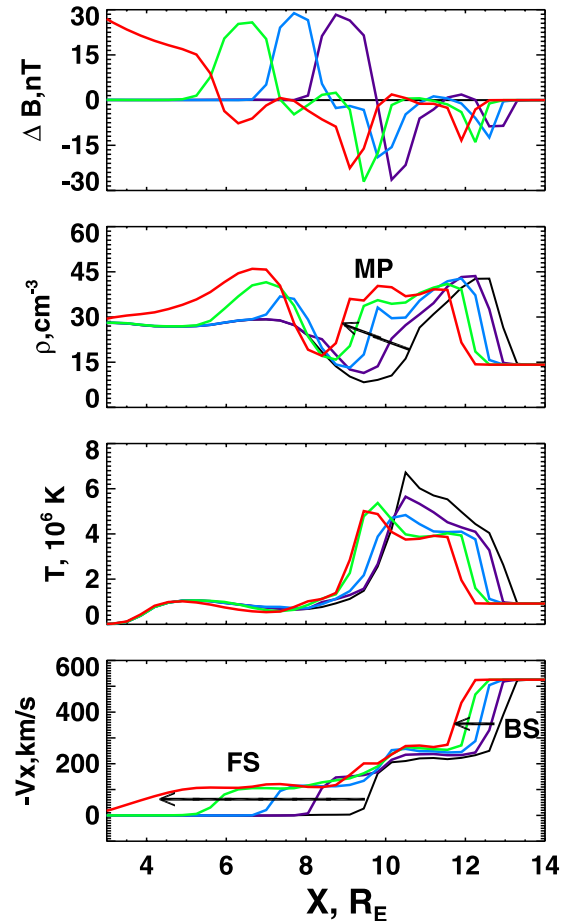


Figure 3. The same parameters as in Figure 3 are shown in next set of times. Black, violet, blue, green and red colors correspond to $t = 135, 150, 165, 180, 195$ s.

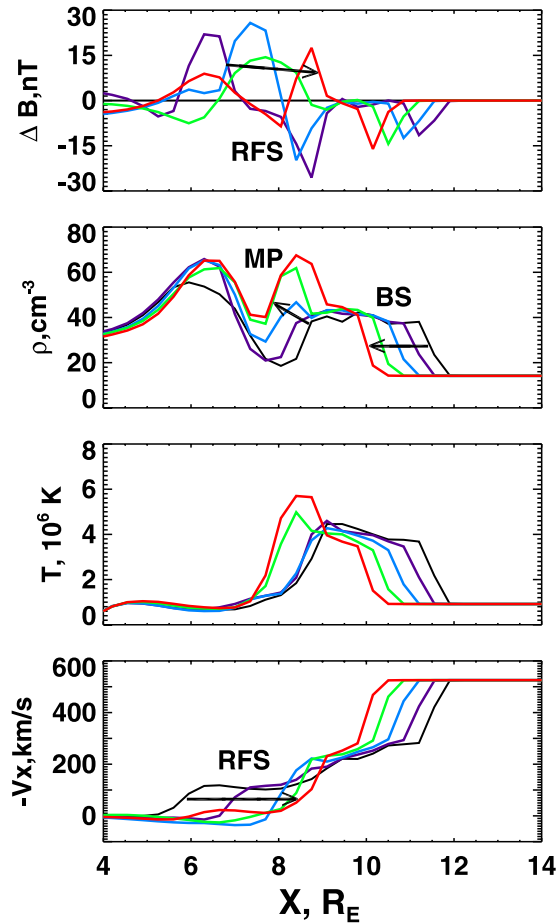


Figure 4. The same parameters as in Figure 2 are shown in next set of times. Black, violet, blue, green and red colors correspond to $t = 210, 225, 240, 255, 270$ s. RFS means a fast shock reflected from the inner numerical boundary.

[16] Figure 5 shows the results of an effort to use profiles of the MHD parameters and the electric current density along the Sun-Earth line to determine the locations of the MP, BS, FS, and RFS as a function of time. We can usually identify the locations of shocks and the magnetic field rotations that mark the magnetopause as local maxima in the current density. Jumps in the flow velocity confirm shock locations. The figure clearly demonstrates that the passage of the FS sets the BS and MP moving inward. The FS reaches the inner boundary near $t = 03:15$, at which time the RFS appears and begins moving outward. When the RFS interacts with the MP, the inward velocity of the MP diminishes. The passage of the RFS sets the BS moving outward. The interaction of the RFS with the MP launches a secondary fast compressional wave moving inward into the magnetosphere (shown by blue stars). Similarly, the interaction of the RFS with the bow shock launches a secondary rarefaction wave moving Earthward in the magnetosheath (shown by blue x's). Throughout these interactions, the MP continues to move inward, only beginning to move outward following its interaction with the secondary fast compressional wave reflected from the inner boundary.

[17] The time interval between interactions FS-MP and RFS-MP is about 2 min, while that between interactions

FS-BS and RFS-BS is a little less than 4 min. The secondary shock propagates from the MP to the inner boundary and returns in about 1.5 min. We estimate the initial FS velocity in the outer magnetosphere to be equal to ~ 600 km s $^{-1}$. However, Rankine-Hugoniot conditions predict the velocity of the same FS in the outer magnetosphere immediately after the interaction with the MP to be a factor of 2–3 greater. The reason for the discrepancy seems to be the inability of the global MHD model to predict some parameters in the magnetosphere, in particular the plasma density. We will present and discuss parallel calculations from another MHD model later.

[18] Figure 6 shows the evolution of the density in the equatorial plane. Each panel presents the change in density, $\Delta\rho$, over 15 s intervals. The density increases in regions traversed by the IP shock and FS. The density decreases (blue arc) where the BS moves inward. This decrease begins near the subsolar point and then extends toward the flanks. Estimations obtained from the Rankine-Hugoniot relations, observations [Koval *et al.*, 2005] and MHD numerical results [Samsonov *et al.*, 2006] show that the velocity of the FS in the dayside magnetosheath is smaller than that in the solar wind. However, it becomes significantly greater in the magnetosphere because of the larger Alfvén velocity there. As shown in Figure 6, this distorts the FS front following its interaction with the BS. This result contradicts with the previous predictions of the gasdynamic model [Spreiter and Stahara, 1995].

[19] The FS encounters the subsolar MP at $t \simeq 02:00$. The shape of the FS in the magnetosphere can be seen in at $t = 03:00-02:45$, where the blue region at $x \simeq 8 R_E$ represents a density decrease in the outer magnetosphere associated with the inward motion of outer magnetospheric plasma. Slightly radially outward from this location, densities increase (red) as the magnetopause itself moves inward. The FS reaches

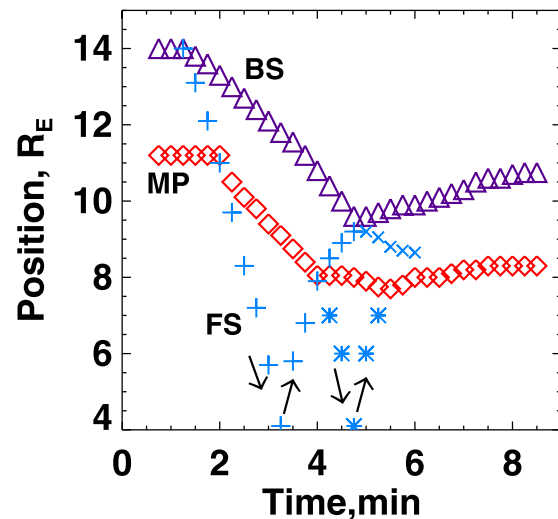


Figure 5. Positions of the subsolar magnetopause and bow shock in dependence on time are shown by red squares and violet triangles, the motion of forward fast shock and reflected fast shock is shown by blue crosses, the motion of secondary reflected fast shock is shown by blue stars. See details in text.

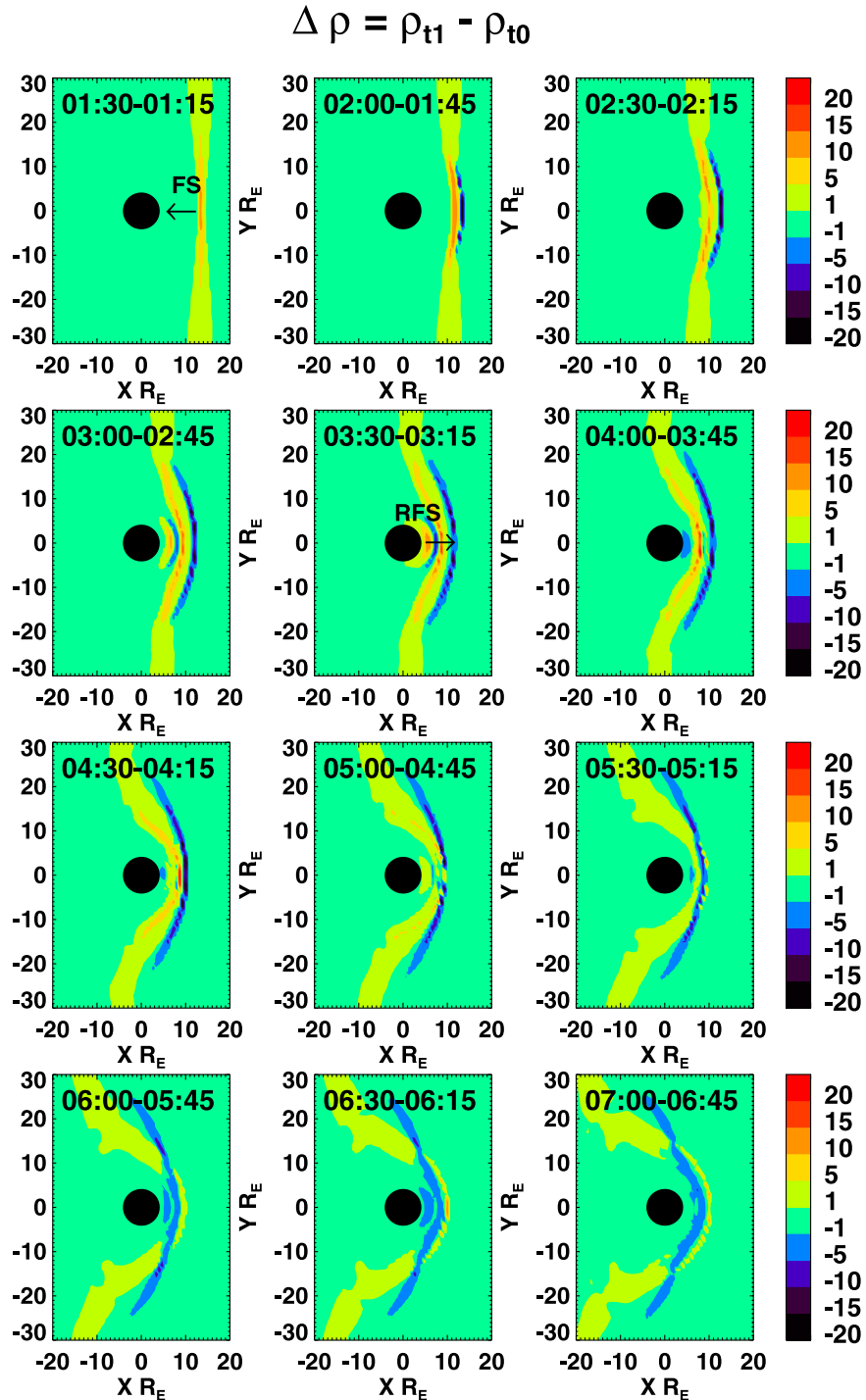


Figure 6. Contours of $\Delta \rho$ in the equatorial plane for a set of time intervals, where $\Delta \rho = \rho_{t1} - \rho_{t0}$ is a variation of density during 15 s interval. Plasma flow cannot penetrate inside the black circle around $(0, 0)$, therefore the fast shock would reflect in the dayside region and moves outward as a RFS.

the inner numerical boundary (the black circle centered on $(x, y) = (0, 0)$) at $t = 03:15$, after which time contours for the density variations begin moving sunward. The RFS front is strongest in the vicinity of the Sun-Earth line. Plates $t = 04:00-03:45$, $04:30-04:15$, and $05:00-04:45$ illustrate the outward propagation of the RFS through the magnetosphere and magnetosheath to the BS. Once the RFS reaches the

bow shock, the latter boundary begins moving outward. The density decreases (blue) associated with inward motion are replaced by density increases (yellow) associated with outward motion. The density increases begin in the subsolar region and subsequently spread toward the flanks, consistent with a wave on the bow shock propagating antisunward.

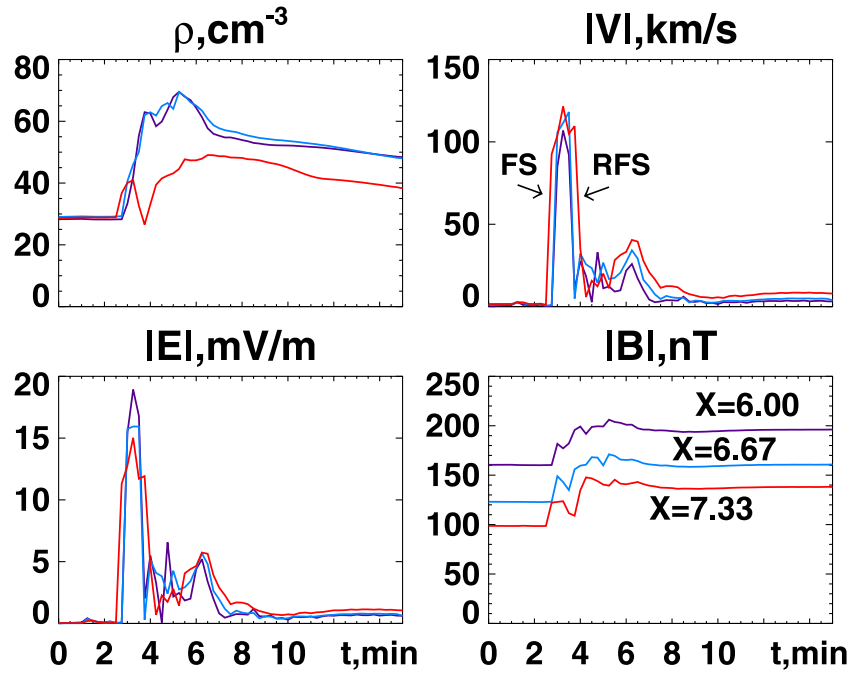


Figure 7. Temporal variations of the density, velocity, electric and magnetic fields in three points ($X = 6.0, 6.67, 7.33 R_E$) at the Sun-Earth line (i.e., what would be observed by a virtual spacecraft). FS and RFS mark the moments when the forward and reflected fast shocks pass the point of observation.

Šafránková *et al.* [2007] recently reported observations of such structures in Geotail and Interball data.

[20] Figure 7 shows the time variations of several MHD parameters in the magnetosphere at three points along the Sun-Earth line. The arrival of the fast shock results in density, velocity, electric and magnetic field enhancements at 02:30. Velocities increase to 100 km s^{-1} , while electric fields increase to more than 15 mV m^{-1} . The arrival of the reflected shock near on one minute later results in abrupt decreases in the velocity and electric field, but changes are less obvious in the density and magnetic field strength. Very similar profiles can be seen at all three locations, with the magnitude of the electric field pulse increasing toward the Earth due to greater magnetic field strengths there.

[21] These results demonstrate the reflection of a FS from the inner numerical boundary of the global MHD model. Ridley *et al.* [2006] associated this reflection boundary with the plasmopause (PP). This assumption is not well founded yet. Therefore we explore the interaction of incident shock waves with the PP using another numerical MHD model in the next section.

4. Where Does the Interplanetary Shock Really Reflect?

[22] In the real magnetosphere, waves incident upon the plasmopause are reflected and transmitted. To simulate the propagation of a shock wave in the magnetosphere, we employ the usual conservative MHD equations and consider a one-dimensional problem with velocities solely along the Sun-Earth line (x -axis) and magnetic fields strictly transverse to this line. We use the model magnetic field strengths [Tsyganenko, 2002a, 2002b] and densities [Carpenter and

Anderson, 1992] for the initial conditions. To ensure a quasi-static equilibrium, we invoke

$$\frac{1}{4\pi}(\nabla \times \mathbf{B}) \times \mathbf{B} = \nabla p, \quad (1)$$

and $p = nkT$ to determine the temperature and thermal pressure. The inner and outer boundaries of the simulation lie at $x = 4$ (in the plasmasphere) and $10 R_E$ (in the outer magnetosphere). The plasmopause initially lies at $x = 6.1 R_E$, where the density varies from 157 to 10 cm^{-3} . Dashed lines in Figure 8 illustrate initial profiles for the density, velocity, thermal pressure, and magnetic field strength.

[23] We initiate the interaction of an Earthward-propagating FS with the magnetosphere by imposing jumps in all the MHD parameters in the outer magnetosphere (at $x = 10 R_E$). This shock is several times stronger than in the global simulation above. The interaction of the FS with the PP displaces the PP inward and results in both a transmitted FS going into the plasmasphere and a sunward-moving RFS. Solid lines in Figure 8 indicate the profiles for the various parameters shortly after the FS-PP interaction, while labels indicate the locations of the FS, PP, and RFS. The RFS moves outward at speeds greater than those at which the FS moves inward because Alfvén velocities are much greater in the outer magnetosphere than in the plasmasphere [e.g., Moore *et al.*, 1987; Lee and Hudson, 2001]. The PP moves Earthward after the interaction at a speed nearly half that of the velocity of the transmitted FS. We have reproduced these results in separate simulations for weaker (but more realistic) incoming FS. We do not observe significant attenuation of the shocks during their propagation in the

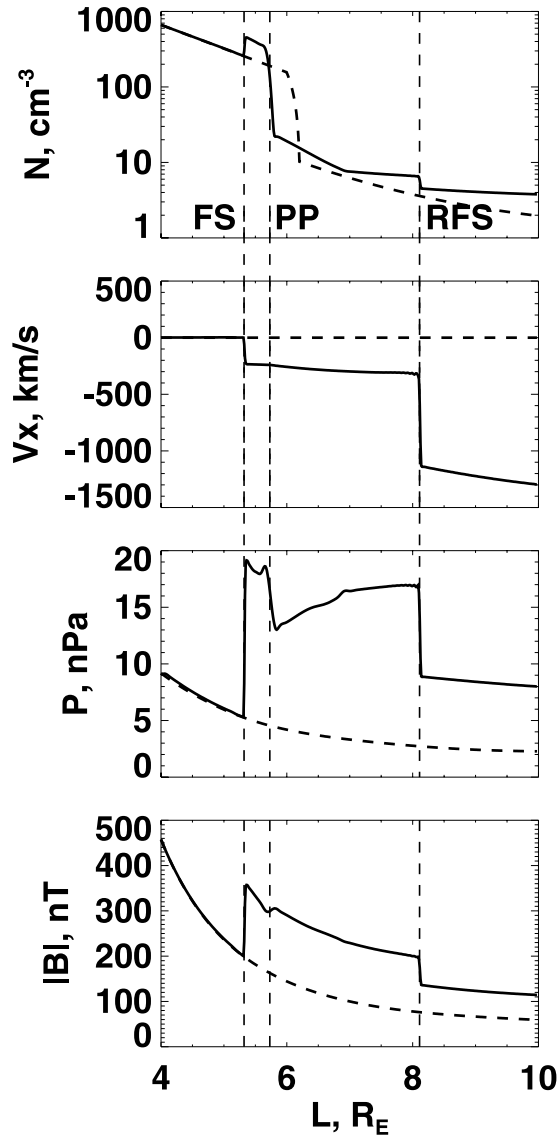


Figure 8. Profiles of density, velocity, thermal pressure, and magnetic field at the Sun-Earth line obtained using a one-dimensional MHD model. Dashed lines correspond to the initial quasi-static configuration, solid lines correspond to the numerical results at a moment shortly after the interaction of the fast shock (FS) with the plasmapause (PP). Part of energy of the FS goes into the plasmasphere, and part of energy reflects from the PP and propagates sunward as a reflected fast shock (RFS).

magnetosphere and plasmasphere despite strong magnetic field and density gradients there. In the absence of any distinct boundaries between the plasmasphere and the ionosphere, the fast shock transmitted into the plasmasphere must reach the ionosphere and cause the well-known sudden impulse signature at low-latitudes.

5. Estimations Obtained From the Numerical Results and Comparison With Observations

[24] We can approximately calculate the energy transmitted along the Sun-Earth line. The total energy flux in the

MHD equations is

$$\mathbf{q} = \mathbf{v} \left(\frac{\rho V^2}{2} + \frac{\gamma}{\gamma - 1} p \right) + \frac{1}{4\pi} [\mathbf{B} \times (\mathbf{v} \times \mathbf{B})]. \quad (2)$$

[25] The interaction of the IP shock with the bow shock results in the transmission of both the FS and the SEW-CD-SS combination into the magnetosheath. Both sets of discontinuities transmit energy into the magnetosheath. Using the Rankine-Hugoniot conditions and the results of *Samsonov et al.* [2006], we can estimate the energy flux of the solar wind flow downstream of the FS. The energy flux of the transmitted FS in the magnetosheath is 92% that of the initial IP shock. The SEW-CD-SS energy is 8% respectively.

[26] The interaction of the FS with the magnetopause results in the transmission of a FS and the reflection of a FEW. Using the Rankine-Hugoniot conditions for the same model shock, we find that 80% of the energy incident on the magnetopause enters the magnetosphere, corresponding to 74% of the energy associated with the initial IP shock. The final interaction occurs at the plasmapause. Using the results shown in Figure 8, we find that 69% of the energy incident on the plasmapause crosses that boundary and may reach the ionosphere. If the results for this strong IP shock typify those for weaker shocks, our results indicate that the FS transmitted through the bow shock, magnetopause, and plasmapause ultimately contains only 51% of the energy flux of the initial IP shock.

[27] Considering transmission of the FS into the magnetosphere and plasmasphere, one remark should be taken into account. According to the Rankine-Hugoniot conditions, the tangential discontinuity (MP) exists both before and after the interaction with the FS. It means that there is no penetration of the solar wind plasma into the magnetosphere. Strictly speaking, we have no transmitted shock, but a new FS appearing at the moment of interaction. However, we can speak about transmission of energy through the magnetopause.

[28] Secondary waves resulting from multiple reflections complicate the picture. The SEW-CD-SS combination may transmit more energy into the magnetosphere, while the interaction of the RFS with the magnetopause results in another fast mode wave moving Earthward and so on. Some of the energy associated with the compressional waves propagating across L shells will be lost via mode coupling to transverse waves at inhomogeneities [*Tamao*, 1964]. The transverse waves transmit energy to the high-latitude ionosphere.

[29] The interaction of the FS with the ionosphere lies beyond the scope of this paper, but we can make some simple estimates of propagation velocities and lag times. *Lee and Hudson* [2001] demonstrated that the abrupt variations in the solar wind dynamic pressure responsible for sudden impulses should also excite periodic compressional waves in the plasmasphere, which requires multiple wave reflections from the ionosphere and the plasmapause. As noted by *Tamao* [1964] and *Ohnishi and Araki* [1992], the shielding effect of ionospheric currents can reflect incident fast MHD waves. We can compare rough estimates for the time needed for a disturbance moving at the Alfvén velocity to propagate along the Sun-Earth line along the

MP-PP-MP and MP-ionosphere-MP paths. The first time is ~ 1 min for a mean Alfvén velocity of 1000 km s^{-1} , while the second is ~ 3 min for a mean Alfvén velocity in the plasmasphere of 500 km s^{-1} . For comparison, recall the results from the global MHD simulation discussed above, namely that the shock propagates from the MP to the inner boundary at $x \simeq 3 R_E$ and back in approximately 2 min.

[30] Observations in the outer magnetosphere near noon are consistent with the model predictions presented in this paper. Useful information can be extracted from geosynchronous electric field measurements. As shown in Figure 7, the global simulation predicts that the sequential arrival of the FS and RFS results in a strong electric field pulse with a duration about 1–2 min. Knott *et al.* [1982, 1985] reported two such structures connected with IP shocks in the magnetosphere. In the first case, the dawnward electric field was 17 mV m^{-1} , while in the second case it was 7 mV m^{-1} . The durations of the pulses were about 1.5 min (ending with a magnetopause crossing in the first case). The observed dawnward electric fields indicate that the passage of FS initiates transient earthward plasma flows.

[31] Figure 6 of Andreeva and Prech [2007] presents GOES-8 and GOES-10 observations of the dayside geosynchronous magnetic field following the arrival of an IP shock. The magnetic field magnitude first increases abruptly, then decreases slightly, and finally increases more gradually 1.5–2 min later. Figure 6 of Russell *et al.* [1999] presents GOES-10 observations of the dayside magnetosphere indicating a very similar response to a different IP shock.

[32] In both cases, we attribute the first abrupt increase to the forward FS and the second more gradual increase to the RFS. As discussed above, the reflection may occur at either the plasmopause or the ionosphere. Since the plasmopause lies only a few Earth radii away from the geosynchronous orbit near noon and the shock propagates at velocities greater than the large Alfvén velocity in the outer magnetosphere, the difference in arrival times between the FS and an RFS reflected from the plasmopause should be on the order of seconds or tens of seconds. By contrast, the time difference between the arrival times of the FS and an RFS reflected from the ionosphere should be 2–3 min. We conclude that the geosynchronous observations are consistent with a strong reflection of the FS from the ionosphere (and only a weak reflection from the plasmopause).

[33] We can exclude the possibility that the two-step increase in the geosynchronous magnetic field results from the arrival of the FS and then the set of SEW-CD-SS discontinuities. The global MHD model does not predict this scenario. Furthermore, the Rankine-Hugoniot conditions predict that the MP moves inward nearly as fast as the 200 km s^{-1} SEW-CD-SS propagation velocity in the magnetosheath. Consequently, the SEW-CD-SS does not reach the MP until the MP stops due to its interaction with the RFS.

6. Conclusions

[34] We used MHD simulations to study the interaction of IP shocks with the Earth’s magnetosphere. Like Samsonov *et al.* [2006], we considered a moderately strong IP shock with a density compression ratio $\rho_2/\rho_1 = 2.84$ propagating

strictly antisunward in a solar wind flowing radially outward from the Sun.

[35] The initial interaction of the IP shock with the Earth’s bow shock sets the bow shock moving inward and launches a FS into the magnetosheath and a set of SEW-CD-SS discontinuities. Because the velocity of the FS in the magnetosheath is less than that in the upstream solar wind, the originally planar shock front becomes distorted. The SEW-CD-SS discontinuities essentially move Earthward with the magnetosheath flow velocity. Once the transmitted FS interacts with the MP, a forward FS appears in the magnetosphere and a reflected FEW appears in the magnetosheath. In addition, the MP begins to move Earthward.

[36] The inner numerical boundary of the global magnetospheric BATS-R-US code is a sphere with a radius of about $3 R_E$. The FS reflects from this boundary, and a RFS propagates outward through the dayside magnetosphere and magnetosheath. The reflected shocks terminate the inward motion of the MP and BS. Because the global magnetospheric code does not incorporate a self-consistent plasmasphere, the results obtained from the simulation may not describe the real situation well.

[37] We therefore presented a supplementary 1-D MHD model for conditions along the Sun–Earth line to simulate the interaction of the FS with a more realistic plasmopause. We find that most of the FS energy penetrates into the plasmasphere and that only a relatively small fraction (our estimate: $\sim 30\%$ of the incoming FS energy) is reflected. This is consistent with the FS reaching the ionosphere and producing the well-known sudden impulse in ground observations.

[38] However, in situ observations provide increasing evidence for a strong reflected fast mode wave (RFS). Following the arrival of IP shocks, the bow shock moves inward and then outward, and there is a two step response in the geosynchronous magnetic field strength accompanied by a dawnward electric field pulse. Our calculations and timing considerations suggest that the FS reflects from the dayside ionosphere and that the RFS propagates through the magnetosphere and magnetosheath to reach the bow shock, in qualitative agreement with predictions of the global MHD code. A joint analysis of high-resolution data at the subsolar bow shock and magnetopause, and in the subsolar magnetosphere (particularly flow velocities and electric fields) in conjunction with low-latitude ground observations of sudden impulse signatures would help to confirm or disprove our suggestions.

[39] **Acknowledgments.** The work was supported by NASA’s MMS project and partly by “Russian Scientific School” president grant 760.2003.5 and Program RNP.2.2.2.2.2190 “Intergeophysica”. Simulation results have been provided by the Community Coordinated Modeling Center (CCMC) at Goddard Space Flight Center through their public Runs on Request system (<http://ccmc.gsfc.nasa.gov>). The CCMC is a multiagency partnership between NASA, AFMC, AFOSR, AFRL, AFWA, NOAA, NSF and ONR. We thank Masha Kuznetsova for useful comments in preparation for the simulation. In particular, we have studied the run “*Andrey_Samsonov_111706_1*”. The BATS-R-US Model was developed by the CSEM group at the University of Michigan. Haje Korth provided the IDL Geopack DLM used in this paper.

[40] Zuyin Pu thanks the reviewers for their assistance in evaluating this paper.

References

Andreeva, K., and L. Prech (2007), Propagation of interplanetary shocks into the Earth’s magnetosphere, *Adv. Space Res.*, doi:10.1016/j.asr.2007.04.079.

- Araki, T. (1994), A Physical Model of the Geomagnetic Sudden Commencement, in *Solar Wind Sources of Magnetospheric Ultra-Low-Frequency Waves*, *Geophys. Monogr. Ser.*, vol. 81, edited by M. J. Engebretson, K. Takahashi, and M. Scholer, pp. 183–200, AGU.
- Carpenter, D. L., and R. R. Anderson (1992), An ISEE/Whistler model of equatorial electron density in the magnetosphere, *J. Geophys. Res.*, *97*, 1097–1108.
- De Zeeuw, D. L., S. Sazykin, R. A. Wolf, T. I. Gombosi, A. J. Ridley, and G. Tóth (2004), Coupling of a global MHD code and an inner magnetospheric model: Initial results, *J. Geophys. Res.*, *109*, A12219, doi:10.1029/2003JA010366.
- Dryer, M. (1973), Bow shock and its interaction with interplanetary shocks, *Radio Sci.*, *8*(11), 893–901.
- Dryer, M., D. L. Merritt, and P. M. Aronson (1967), Interaction of a plasma cloud with the Earth's magnetosphere, *J. Geophys. Res.*, *72*(11), 2955–2962.
- Gombosi, T. I., D. L. de Zeeuw, K. G. Powell, et al. (2003), Adaptive Mesh Refinement for Global Magnetohydrodynamic Simulation, in *Space Plasma Simulation, Lecture Notes in Physics*, vol. 615, edited by J. Büchner, C. Dum, and M. Scholer, pp. 247–274, Berlin Springer Verlag.
- Grib, S. A. (1972), The interaction of solar wind shock waves with the magnetosphere of the Earth, *Rep. Belorussian Acad. Sci.*, *16*, 493–496.
- Grib, S. A. (1973), Some questions of interaction of shock waves of solar wind with the magnetosphere of the Earth, *Geomagn. Aeron.*, *13*, 788–793.
- Grib, S. A. (1982), Interaction of non-perpendicular/parallel solar wind shock waves with the earth's magnetosphere, *Space Sci. Rev.*, *32*, 43–48.
- Grib, S. A., and E. A. Pushkar (2006), Asymmetry of nonlinear interactions of solar MHD discontinuities with the bow shock, *Geomagn. Aeron.*, *46*, 417–423.
- Grib, S. A., B. E. Briunelli, M. Dryer, and W.-W. Shen (1979), Interaction of interplanetary shock waves with the bow shock-magnetopause system, *J. Geophys. Res.*, *84*, 5907–5921.
- Guo, X.-C., Y.-Q. Hu, and C. Wang (2005), Earth's magnetosphere impinged by interplanetary shocks of different orientations, *Chinese Phys. Lett.*, *22*, 3221–3224, doi:10.1088/0256-307X/22/12/067.
- Ivanov, K. G. (1964), Interaction of running shock waves with strong discontinuities in the space vicinity of the Earth, *Geomagn. Aeron.*, *4*, 803–806.
- Knott, K., D. Fairfield, A. Korth, and D. T. Young (1982), Observations near the magnetopause at the onset of the July 29, 1977, sudden storm commencement, *J. Geophys. Res.*, *87*, 5888–5894.
- Knott, K., A. Pedersen, and U. Wedeken (1985), GEOS 2 electric field observations during a sudden commencement and subsequent substorms, *J. Geophys. Res.*, *90*, 1283–1288.
- Koval, A., J. Safránková, Z. Nemeček, L. Přech, A. A. Samsonov, and J. D. Richardson (2005), Deformation of interplanetary shock fronts in the magnetosheath, *Geophys. Res. Lett.*, *32*, L15101, doi:10.1029/2005GL023009.
- Koval, A., J. Safránková, Z. Nemeček, A. A. Samsonov, L. Přech, J. D. Richardson, and M. Hayosh (2006), Interplanetary shock in the magnetosheath: Comparison of experimental data with MHD modeling, *Geophys. Res. Lett.*, *33*, L11102, doi:10.1029/2006GL025707.
- Lee, D.-H., and M. K. Hudson (2001), Numerical studies on the propagation of sudden impulses in the dipole magnetosphere, *J. Geophys. Res.*, *106*, 8435–8446, doi:10.1029/2000JA000271.
- Moore, T. E., D. L. Gallagher, J. L. Horwitz, and R. H. Comfort (1987), MHD wave breaking in the outer plasmasphere, *Geophys. Res. Lett.*, *14*, 1007–1010.
- Nishida, A. (1978), *Geomagnetic diagnosis of the magnetosphere*, Physics and Chemistry in Space, Springer, New York.
- Ohnishi, H., and T. Araki (1992), Two-dimensional interaction between a plane hydromagnetic wave and the earth-ionosphere system with curvature, *Annales Geophysicae*, *10*, 281–287.
- Powell, K. G., P. L. Roe, T. J. Linde, T. I. Gombosi, and D. L. de Zeeuw (1999), A solution-adaptive upwind scheme for ideal magnetohydrodynamics, *J. Comput. Phys.*, *154*, 284–309.
- Pushkar, E. A., A. A. Barmin, and S. A. Grib (1991), MHD-approximation study of the incidence of the solar wind shock on the Earth's bow shock, *Geomagn. Aeron.*, *31*, 522–525.
- Ridley, A. J., D. L. de Zeeuw, W. B. Manchester, and K. C. Hansen (2006), The magnetospheric and ionospheric response to a very strong interplanetary shock and coronal mass ejection, *Adv. Space Res.*, *38*, 263–272, doi:10.1016/j.asr.2006.06.010.
- Russell, C. T., X. W. Zhou, P. J. Chi, H. Kawano, T. E. Moore, W. K. Peterson, J. B. Cladis, and H. J. Singer (1999), Sudden compression of the outer magnetosphere associated with an ionospheric mass ejection, *Geophys. Res. Lett.*, *26*, 2343–2346, doi:10.1029/1999GL900455.
- Samsonov, A. A., Z. Nemeček, and J. Safránková (2006), Numerical MHD modeling of propagation of interplanetary shock through the magnetosheath, *J. Geophys. Res.*, *111*, A08210, doi:10.1029/2005JA011537.
- Shen, W.-W., and M. Dryer (1972), Magnetohydrodynamic theory for the interaction of an interplanetary double-shock ensemble with the Earth's bow shock, *J. Geophys. Res.*, *77*(25), 4627–4644.
- Song, P., D. L. DeZeeuw, T. I. Gombosi, C. P. T. Groth, and K. G. Powell (1999), A numerical study of solar wind-magnetosphere interaction for northward interplanetary magnetic field, *J. Geophys. Res.*, *104*, 28,361–28,378.
- Spreiter, J. R., and S. S. Stahara (1995), The location of planetary bow shocks: A critical overview of theory and observations, *Adv. Space Res.*, *15*, 433–449.
- Tamao, T. (1964), The structure of three-dimensional hydromagnetic waves in a uniform cold plasma, *J. Geomag. Geoelect.*, *18*, 89–114.
- Tsyganenko, N. A. (2002a), A model of the near magnetosphere with a dawn-dusk asymmetry 1. Mathematical structure, *J. Geophys. Res.*, *107*(A8), 1179, doi:10.1029/2001JA000219.
- Tsyganenko, N. A. (2002b), A model of the near magnetosphere with a dawn-dusk asymmetry 2. Parameterization and fitting to observations, *J. Geophys. Res.*, *107*(A8), 1176, doi:10.1029/2001JA000220.
- Safránková, J., Z. Nemeček, L. Přech, A. A. Samsonov, A. Koval, and K. Andreceva (2007), Modification of interplanetary shock near the bow shock and through the magnetosheath, *J. Geophys. Res.*, *112*, A08212, doi:10.1029/2007JA012503.
- Yan, M., and L. C. Lee (1996), Interaction of interplanetary shocks and rotational discontinuities with the Earth's bow shock, *J. Geophys. Res.*, *101*, 4835–4848, doi:10.1029/95JA02976.
- Zhuang, H. C., C. T. Russell, E. J. Smith, and J. T. Gosling (1981), Three-dimensional interaction of interplanetary shock waves with the bow shock and magnetopause - A comparison of theory with ISEE observations, *J. Geophys. Res.*, *86*, 5590–5600.

J. Imber, University of Oxford, Oxford OX1 3RH, UK.

A. A. Samsonov, Department of Earth Physics, Institute of Physics, St. Petersburg State University, St. Petersburg, 198504, Russia. (samsonov@geo.phys.spbu.ru)

D. G. Sibeck, NASA Goddard Space Flight Center, Greenbelt, MD 20771, USA.